

Remote-sensing techniques for analysing landslide kinematics: a review

CHRISTOPHE DELACOURT¹, PASCAL ALLEMAND², ETIENNE BERTHIER³, DANIEL RAUCOULES⁴,
BÉRANGÈRE CASSON², PHILIPPE GRANDJEAN², CLAUDE PAMBRUN⁵ and ERIC VAREL⁶

Key words. – Remote sensing, Landslide, Surface displacement, InSAR, Image correlation

Abstract. – Surface displacement field of landslides is a key parameter to access to their geometries and mechanical properties. Surface displacements can be calculated using remote-sensing methods such as interferometry for radar data and image correlation for optical data. These methods have been elaborated this last decade and successfully applied on sensors (radar, cameras, terrestrial 3D laser scanner imaging) either attached to space or aerial platforms such as satellites, planes, and unmanned radio-controlled platforms (drones and helicopters) or settled at fixed positions emplaced in the front of landslides. This paper reviews the techniques of image analysis (interferometry and optical data correlation) to measure displacements and examines the performance of each type of platforms. Examples of applications of these techniques in French South Alps are shown. Depending on the landslide characteristics (exposure conditions, size, velocity) as well as the goal of the study (operational or scientific purpose), one or a combination of several techniques and data (characterized by several resolution, accuracy, covered surface, revisiting time) have to be used. Radar satellite data processed with differential interferometric or PS methods are mainly suitable for scientific purposes due to various application limitations in mountainous area. Optical satellite and aerial images can be used for scientific studies at fairly high resolution but are strongly dependant on atmospheric conditions. Platforms and sensors such as drone, fixed camera, fixed radar and Lidar have the advantage of high adaptability. They can be used to obtain very high resolution and precise 3D data (of centimetric accuracy) suitable for both scientific and operational purposes.

Utilisation de techniques de télédétection pour l'analyse de la cinématique de glissements de terrain

Mots clés. – Télédétection, Glissement de terrain, Déplacement de surface, InSAR, Corrélation d'images

Résumé. – Connaître le champ de déplacement de surface des glissements de terrain est un paramètre clé pour accéder à leurs structures internes ainsi qu'à leurs propriétés mécaniques. Les déplacements de surface peuvent être calculés grâce à des techniques de télédétection telles que l'interférométrie pour les images radar ou la corrélation d'images optiques. Ces méthodes ont été développées au cours de la dernière décennie, et appliquées avec succès à différents capteurs (radar, appareil photos, scanner laser photogrammétrique) embarqués sur des plates-formes spatiales ou aériennes, telles les satellites, les avions et les plates-formes radio-commandées ou fixées à des positions fixes en face des glissements de terrain. Cet article passe en revue ces différentes techniques d'analyses d'images et examine les performances de chaque type de plate-forme. Des exemples d'application de ces techniques sur des glissements situés dans les Alpes françaises du Sud sont présentés. En fonction des conditions d'exposition, de la taille, de la vitesse du glissement et de l'objectif de l'étude (opérationnel ou scientifique), la solution optimale peut se révéler être soit une seule technique ou la combinaison de techniques et de données (caractérisées par différentes résolutions, précisions, surfaces couvertes, temps de revisite). Les techniques interférométriques et PS sont principalement dédiés à des objectifs scientifiques en raison des différentes limitations affectant leur utilisation en zones montagneuses. Les images acquises par des satellites optiques ou lors de missions aériennes peuvent être utilisées pour des objectifs scientifiques mais sont fortement dépendantes des conditions atmosphériques. Les plates-formes et capteurs drone, appareil photos et radar fixes ainsi que Lidar offre l'avantage de la souplesse d'utilisation. Ils fournissent des mesures à très haute résolution spatiale et grande précision (de l'ordre du centimètre) utilisable à la fois pour des objectifs scientifiques et opérationnels.

1. 'Domaines Océaniques' UMR 6538 CNRS-IUEM-UBO, Place Copernic, F-29280, Plouzané, France. Tel. +33 (0)298 498 742 / Fax. +33 (0)298 498 760 / E-mail : christophe.delacourt@univ-brest.fr

2. 'Laboratoire de Sciences de la Terre' UMR 5570 CNRS-UCBL-ENS, 2 Rue Dubois, F-69622, Villeurbanne, France.

3. Laboratoire d'Etudes en Géophysique et Océanographie Spatiales' UMR 5566 CNRS-CNES-UPS-IRD, 14 Avenue Edouard Belin, F-31401, Toulouse cedex 9, France.

4. 'Bureau de Recherches Géologiques et Minières' (BRGM), Aménagement et Risques Naturels, BP 6009, F-45060 Orléans, France.

5. 'Géosciences Azur', UMR 6526 CNRS-UNSA-IRD, 250 Rue Albert Einstein, F-06560, Valbonne Sophia-Antipolis, France.

6. 'ATM3D', Savoie Technolac, BP 269, F-73370 Le Bourget du Lac cedex, France.

Manuscrit déposé le 20 janvier 2006; accepté après révision le 7 mai 2006.

INTRODUCTION

The analysis of the surface velocity field is useful to define the parameters controlling the dynamics of low-velocity landslides (from some centimeters per year over several years to some centimeters per day) for both scientific and hazard related purposes. The range of temporal variability in surface velocity is large including multiyear trend, seasonal (meteorologically-driven) variations, and episodic events [Casson *et al.*, 2003]. Thus, a multitemporal and multiscale study is required to characterize the signature of distinct parameters. Presently, most of the techniques to monitor landslide displacement are derived from the field measurement of the successive positions of reference stations. Conventional geodetic (triangulation, tacheometry) and extensometry techniques remain the most common techniques [Angeli *et al.*, 2000], GPS surveys being an alternative [Jackson *et al.*, 1996; Malet *et al.*, 2002]. The data acquired using these techniques are available only for major landslides and are limited to the last 15 years (GPS) or 20 (laser) years. Moreover, due to spatial and temporal heterogeneities of terrain movements, such ground-based measurements are not accurate enough to fully describe the velocity field of a landslide. Additionally these techniques require additional human intervention on the landslide or at

its vicinity. Remote sensing imagery is a powerful tool to measure landslide displacements because it offers a synoptic view of the landslide that can be repeated at different time intervals. Furthermore this technique is efficient at various scales (from the landslide to regional scale). However, earth observation satellite imagery exists only for about 25 years. Moreover, the spatial resolution of optical satellite imagery systems is typically not adequate for landslide studies until the recent improvements of optical sensors, such as the ones on-board IKONOS, Quickbird or SPOT5. The development of high resolution digital cameras fixed on unmanned platforms that are radio controlled by an operator permits high resolution acquisitions with an adapted temporal frequency. At last, terrestrial photogrammetric laser ranging (or terrestrial 3D laser scanner imaging) sensors produce both topography and orthophotography in a single acquisition with centimeter resolution and precision.

Two main methods of displacement measurements have been developed during these last years, which characteristics are indicated in table I. The first one, differential SAR interferometry (DInSAR), is based on Synthetic Aperture Radar (SAR) data and the second one, image correlation (also called feature tracking), is based on optical data. The development of these techniques is closely related to the development of new platforms and sensors that allow data

TABLE I. – Characteristics of the radar and optical remote-sensing sensors, platforms and techniques for landslides surface displacement measurements.
TABL. I. – Caractéristiques des capteurs radar et optiques, plates-formes et méthodes d'analyse pour mesurer les déplacements de surface de glissements de terrain.

| | Radar sensor | | |
|---------------------|--|--|--------------------------------|
| | Satellite | | Ground-based |
| Technique | DInsar | PS | DInsar |
| Measurement Type | 1D component along the line of sight | | |
| Spatial Resolution | ~10 m | ~10 m | better than 10 cm |
| Accuracy | ~ mm to ~ cm | mm | better than 1 mm |
| Swath | 100 x 100 km | | |
| Temporal resolution | 1 to 178 days | | |
| Archive | ERS (1991-2001); JERS (1992-1998); RADARSAT (1995); ENVISAT (2002) | | |
| Major references | Fruneau <i>et al.</i> [1996]; Rott <i>et al.</i> [1999]; Kimura and Yamaguchi [2000]; Squarzoni <i>et al.</i> [2003]; Strozzi <i>et al.</i> [2005] | Ferretti <i>et al.</i> [2001]; Colesanti <i>et al.</i> [2003]; Hilley <i>et al.</i> [2004] | Antonello <i>et al.</i> [2004] |

| | Optical sensor | | | |
|---------------------|---|--|--------------------------|-----------------------|
| | Satellite | Aerial | Remote-controlled | Fixed Camera |
| Measurement Type | 2 D horizontal displacement or 3D if DEMs available | | | |
| Spatial Resolution | 0.6 m to 80 m | 0.5 m to 2 m | < mm to 1 m | ~ cm to ~ m |
| Accuracy | ~1/5 to 1 pixel | 2-3 pixels | A few pixels | 1/5 pixel |
| Swath | 10 x 10 km to 60 x 60 km | 5 x 5km | 10 x 10 m to 300 x 300 m | 10 x 10 m to 1 x 1 km |
| Temporal resolution | ~30 days | 5-7 years for France | On request | 1 s to 1 day |
| Archive | SPOT1-4 (1986); SPOT5 (2002); IKONOS (1999); QUICKBIRD (1999) | 1950 - ongoing for France | | |
| Major references | Scambos <i>et al.</i> [1992]; Käab [2002]; Käab <i>et al.</i> [2005]; Berthier <i>et al.</i> [2005, 2006] | Käab <i>et al.</i> [2002]; Casson <i>et al.</i> [2003]; Delacourt <i>et al.</i> [2005] | | |

acquisitions at a time-frame that is suited to the landslide velocities. In this paper, DInSAR and optical correlation for displacement measurement are described, and their potential and limitations are compared. Then, the platforms and sensors used for data acquisition are reviewed. At last, the specific use of each type of data is discussed. Most of the techniques and developments described in this paper have been tested and validated on the “La Clapière” landslide, located in the Mercantour massif, on the left bank of the Tinée River (France). The lateral extent of the landslide is about 1300 m, its vertical reaches 650 m. The volume of the landslide has been estimated to 50.10^6 m^3 of Hercynian metamorphic and migmatic rocks. Average velocity over the last thirty years is $\sim 1 \text{ cm.day}^{-1}$ with velocity picks of 30 cm.day^{-1} [Follacci *et al.*, 1988].

METHODS OF DISPLACEMENT MEASUREMENTS

Differential synthetic aperture radar interferometry (DInSAR)

The SAR interferometry (InSAR) technique relies on the processing of two SAR images of the same portion of the Earth’s surface. These images are obtained either using one antenna onboard a platform that has slightly moved between two acquisitions (“repeat pass” interferometry), or using two antennas onboard the same platform (“single pass” interferometry). In both single pass or and repeat pass interferometry, a Digital Elevation Model (DEM) can be calculated in the case none or very little motion occurs between the acquisitions [Zebker and Goldstein, 1985]. In the repeat pass interferometry method, the detection and the quantification of the ground displacement that occurred between the two acquisitions can be achieved by Differential InSAR (DInSAR). The DInSAR technique provides an image, called differential interferogram, representing the ground motion occurring between the acquisitions with a centimetric accuracy and a decametric resolution [Massonnet *et al.*, 1993]. The displacement is calculated by differentiating the phase component of the two coregistrated SAR images after the removal of the topographic effect. The motion is expressed as a complex signal in which a full

rotation phase (called fringe) is equal to half the radar wavelength. This technique only provides the projection of the total ground displacement vector along the line of sight of the satellite (the incidence angle being 23° to 35° for most satellites). In the case of gently dipping areas, the combination of ascending and descending orbit images allows the retrieval of a second component of the displacement vector [Fialko *et al.*, 2005]. DInSAR technique has been successfully applied for detecting and mapping surface displacements caused by natural and anthropic phenomena such as earthquake [Massonnet *et al.*, 1993; Zebker *et al.*, 1994], ice stream flow [Goldstein *et al.*, 1993], volcanic activity [Massonnet *et al.*, 1995] and land subsidence [Carnec *et al.*, 1996; Amelung *et al.*, 1999; Raucoules *et al.*, 2006]. The capability of DInSAR in the determination of the velocity field in landslide areas has been demonstrated only in few cases [Fruneau *et al.*, 1996; Carnec *et al.*, 1996; Rott *et al.*, 1999; Kimura and Yamaguchi, 2000; Squarzoni *et al.*, 2003; Strozzi *et al.*, 2005]. Indeed the DInSAR is not adapted to mountainous regions due to severe limitations related to inadequate acquisition geometry, surface state variations and atmospheric artefacts.

Geometrical limitations due to acquisition geometry

Due to its side-looking acquisition mode, SAR images are subjected to geometrical distortions [Schreier, 1993]. Such areas affected by overlays or shadows cannot be imaged by the sensor [Nagler *et al.*, 2002]. Those types of distortions are induced by the topography and more specifically by the local slope along the line of sight of the satellite. A way to overcome this limitation is to combine ascending and descending orbits over the same area. For example, in the French South Alps, 31% of the ground cannot be imaged using ERS satellites on a descending orbit [Delacourt *et al.*, 2003] but combining ascending and descending orbits reduces the masked surface to 7% (fig. 1). However, among the visible area, depending on the local slope, ground spatial resolution ranges 8 meters (for ERS sensors in the most favorable geometry) to several hundred of meters. Thus, depending on the landslide size and orientation, the areas in which the DInSAR method can be applied successfully may be dramatically reduced.

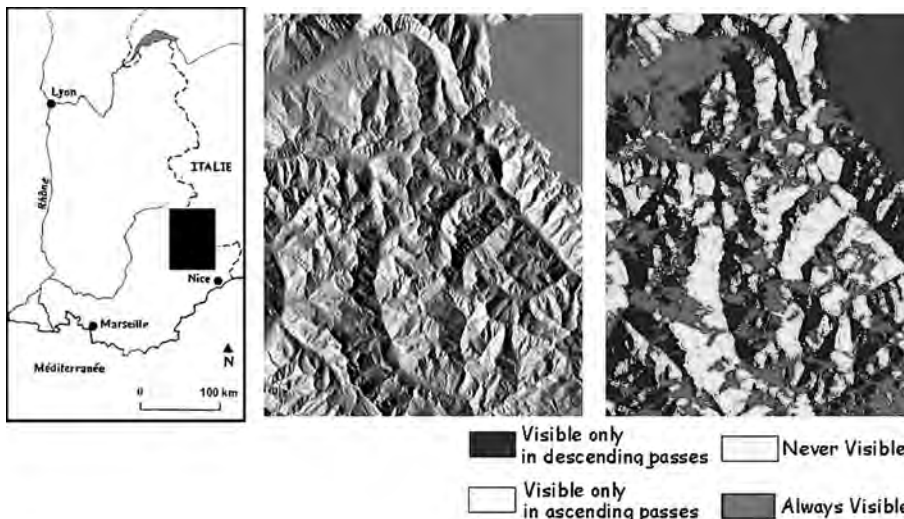


FIG. 1. – Simulation of the geometrical visibility for ERS radar images over the French South Alps. a) The black box corresponds to the extension of the study area. b) Carte de relief (ombrage) de la zone d’étude. c) Carte de visibilité de la zone d’étude.

Limitations due to surface state changes

Temporal changes in the physical or geometrical nature of the soil (vegetation, water content) lead to a decorrelation in radar echoes [Zebker and Villasenor, 1992]. On interferograms, this decorrelation results in noise that masks the surface displacement signal. In most cases, this decorrelation increases in relation with the time span between two acquisitions. Using images acquired by the C-band (5.6 cm wavelength) SAR antenna of ERS-1 satellite over the French South Alps, such a decorrelation occurs after few days below the treeline [Delacourt *et al.*, 2003]. Lack of vegetation contributes to coherence preservation of the images. Then, a compromise has to be found between the loss of correlation and the minimum signal detection. As to the slow landslides, the time span between the two acquisitions has to be large enough in order to detect signal, but it also needs to be short enough to avoid decorrelation. L-band radar images (23.5 cm wavelength), such as the ones that are produced by the JERS-1 satellite (in orbit until 1998), can partly overcome this problem. The L-band signal indeed penetrates deeper into the vegetation cover than the C-band one, providing thus information from more stable scatterers. It is therefore much less sensitive to the temporal decorrelation due to vegetation changes [Strozzi *et al.*, 2003, 2005; Raucoules *et al.*, 2006] (fig. 2). The L-band is particularly suited to investigate decimetric displacements [Strozzi *et al.*, 2004]. In this case, one single interferometric fringe corresponds to a movement of 11.25 cm in the line of sight of the satellite (versus 2.8 cm for the C-band). Therefore, with the L-band, time spans of several months are required to detect displacements of few centimetres occurring due to slow landslides.

Limitations due to atmospheric artefacts

Variation in atmospheric conditions in the lower part of the atmosphere (troposphere) between distinct acquisitions modifies the radar signal time delay, leading to a rotation of the radar signal phase. Then, some tropospheric fringes can be observed on the interferograms [Tarayre and Massonnet, 1996].

Two types of tropospheric artefacts occur in mountain areas. First, a homogeneous change of the atmosphere produces low spatial frequency artefacts that correlate with topography. They can be removed either using a statistical approach [Beauducel *et al.*, 2000], by modeling [Delacourt *et al.*, 1998] or by the measurement of the water content using ancillary satellite data [MODIS, Remi, 2005]. The second type of artefact is due to small-scale local heterogeneities of the troposphere water vapour content [Tarayre and Massonnet, 1996], which produces high frequency artefacts. Due to atmospheric heterogeneities with a horizontal scale from a few tens of meters to a few kilometers, these artefacts might be interpreted as landslide motion signatures (fig. 3). Those artefacts cannot be detected and removed using a single interferogram since most of the atmospheric heterogeneities are not spatially and temporally correlated. The only way to detect and to remove those artefacts is therefore to compare various independent interferograms.

The permanent scatterers method

The permanent scatterers method e.g. PS method [Ferretti *et al.*, 2001] allows to partly overcome the limitations due to the loss of correlation (on areas that are not totally

incoherent) and to atmospheric artefacts. This method identifies permanent scatterers (PS), radar bright and phase stable targets such as buildings, utility poles and rock outcrops within many (more than 20) SAR scenes to determine a time series of displacement with high spatial and temporal resolutions. This technique is widely used in urban areas [Colesanti *et al.*, 2003a, 2003b] where the PS spatial density is of the order of several hundred of benchmarks per square kilometers. Slow moving landslides (few mm/year), located in poorly vegetated areas have been successfully characterized over several years using this technique [Colesanti *et al.*, 2003c; Hilley *et al.*, 2004]. However, in vegetated areas that are characterized by the absence of individual exposed rocks and man made structures, the PS density can drop to zero and the PS technique cannot be applied. Furthermore, PS technique requires that the displacement is at steady state with respect to image sampling. In most of the Alpine landslides, the high temporal and spatial variability of the motion [Squarzoni *et al.*, 2003] will thus limit the systematic application of PS method.

Five main satellites have acquired high amount of radar images, which could be processed in interferometric mode:

- a) the European ERS1-2 (<http://earth.esa.int/ers/>),
- b) the European ENVISAT (<http://envisat.esa.int/>),
- c) the Canadian RADARSAT (<http://radarsat.space.gc.ca/asc/eng/satellites/radarsat1/background.asp>), and
- d) the Japanese JERS (<http://www.eorc.nasda.go.jp/JERS-1/>).

Future of radar satellites

Future radar satellite missions will provide improved spatial resolution. For example RADARSAT2, scheduled to be launched in 2006 (<http://www.radarsat2.info/>), will acquire data with 3 m of resolution. DInSAR technique will thus fail in detecting and mapping surface displacements that are larger than few meters. Indeed, relative displacements that are larger than the quarter of a wavelength between two adjacent pixels (phase aliasing) cannot be measured [Massonnet and Feigl, 1998]. An improvement in the satellite resolution will allow a better assessment of the displacements that are characterized by a small extent or a large gradient. Therefore, it will allow studying a larger range of landslides (and not only the largest and slowest ones).

The Cosmo-Skymed constellation (http://www.asi.it/sito/programmi_cosmo.htm) to be launched in 2007, could address the same issue taking advantage of its short revisiting time span (12 hours in the better case). However, as to the interferometry technique, the X-band sensor of the satellites will be probably less efficient in term of temporal decorrelation than C and L bands: this could be a limitation in the analysis of most of the landslides that are located outside urban regions or in arid areas.

Another perspective in term of new sensors comes from the launch of ALOS (http://www.nasda.go.jp/projects/sat/alos/index_e.html) or TerraSAR-L [Zink, 2003] providing the advantages of a L-band sensor as indicated previously.

Nevertheless, several years will be needed before these missions build an archive that is adequate for multitemporal processing (PS and others). In the next years, those methods will still use ERS-2 (which is presently limited since an attitude problem that occurred in 2001) and ASAR (from the

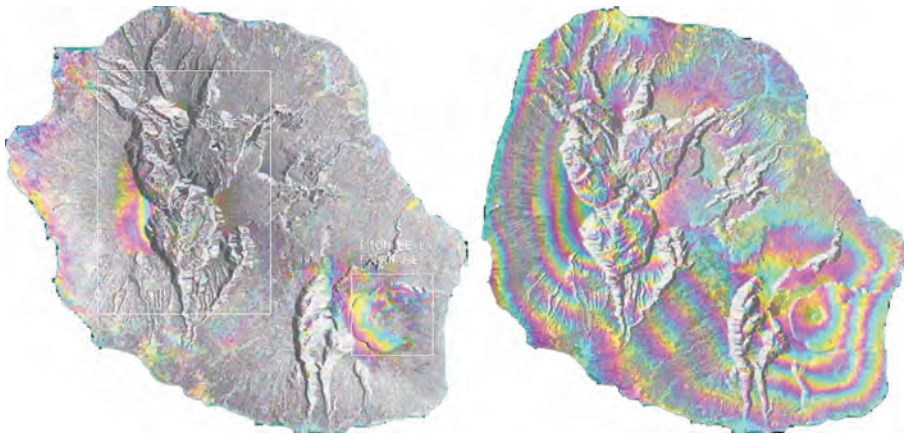


FIG. 2. – Surface changes measurement due to vegetation changes over the Réunion Island on C-band interferometry (left: Radarsat, 2001, 05/15 – 2001, 11/23) and L-band interferometry (right: JERS-1, 1997, 01/02 – 1997, 05/14).

FIG. 2. – Impact de l'évolution de la végétation de l'île de la Réunion sur un interférogramme en bande C (à gauche : RADARSAT, 15/05/2001 – 23/11/2001) et en bande L (à droite : JERS, 02/01/1997 – 14/05/1997).

ENVISAT platform). Ferretti *et al.* (2004) demonstrate a medium compatibility between ERS and ASAR data, which allows PS processing despite slightly different signal frequencies. The ASAR sensor will therefore be able to ensure the data continuity when ERS mission will end.

Fixed radar

A ground based SAR interferometer has been developed since 2000 [Antonello *et al.*, 2004]. The system employed is a semi portable version of the SAR device known as LISA (Linear SAR). It is composed of a few meters long straight track, equipped with a high frequency radar (the nominal wavelength being 1.8 cm). In that case, a full rotation phase corresponds to a motion of 9 mm. The spatial resolution depends on the distance between the radar and the target. A trial of this system on the “Ruinon” landslide (Italy) has been carried out [Antonello *et al.*, 2004]. Over the 18 hours of the measurement survey, a maximum displacement of 9 mm has been observed by LISA. However, due to the high frequency of the radar, this technique is very sensitive to surface state change. C and L band radar version of LISA can be used in order to reduce the loss of coherence.

Correlation of optical data

The 2D displacement field of the Earth surface can be derived by correlating two optical images obtained at different times. This methodology has been applied on aerial and satellite images to measure the displacements generated by earthquakes [Van Puymbroeck *et al.*, 2000], landslides [Delacourt *et al.*, 2004; Casson *et al.*, 2005] and glacier flow [Scambos *et al.*, 1992; Käab, 2002; Käab *et al.*, 2005; Berthier *et al.*, 2005]. The correlated images have to share a common (ground or image) geometry, which is obtained either by orthorectifying both images (the correlation is performed in the ground geometry) or by resampling a secondary image in the geometry of a reference image (correlation performed in the image geometry). A DEM is necessary in both cases and its required accuracy is inversely related to the difference in viewing angles of the correlated images. Ideally, two different DEMs, contemporary to each correlated image, should be used. Over stable areas, the visible ground features should be superimposable on the two successive images. On areas characterized by movements, the visible and recognizable features are shifted by the

displacement. In order to define the ground displacement that occurred between two images, a correlation window of a given width (about 15 to 50 pixels) is defined on the reference (often the oldest) image. The corresponding window is searched on the secondary image by maximizing a correlation function [Vadon and Massonnet, 2000; Baratoux *et al.*, 2001]. The starting point of the search is the expected position of the window as if no displacement occurred between the two acquisitions. The measured shift is directly related to the ground displacement by the pixel size. The main parameters of the calculation are the size of the local window and the maximum displacement expected between the acquisitions. The process is repeated for each pixel of the

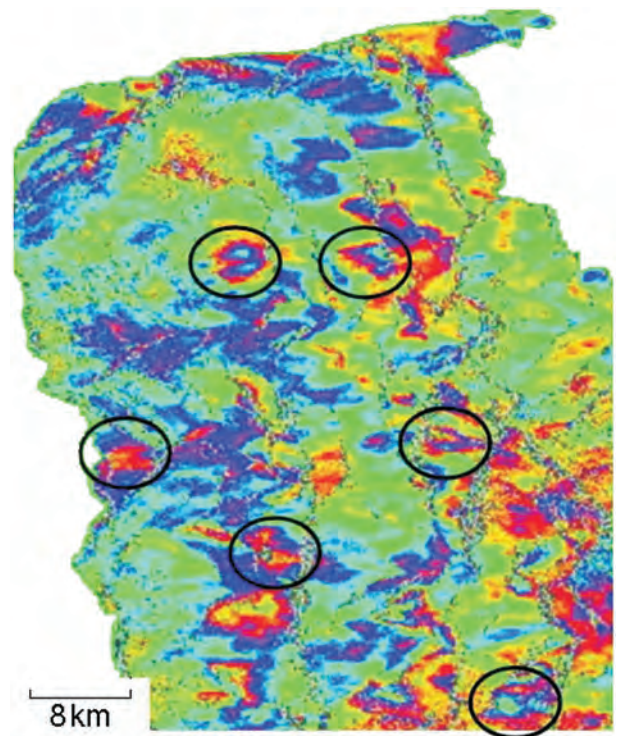


FIG. 3 – Example of bias (black dots) due to tropospheric heterogeneities occurring within 1 day (1995, October 22-23) differential interferogram over the French South Alps.

FIG. 3. – Exemple d'artefacts (cercles noirs) dus à des hétérogénéités troposphériques sur un interférogramme différentiel (22-23 octobre 1995) sur les Alpes françaises du Sud.

oldest image. The result is composed of 3 arrays of the same size as the correlated images. The first array contains the shift in lines for each pixel, the second one contains the shift in columns, and the third one indicates the quality of the correlation. The choice of the size of the correlation window is a compromise between the desired accuracy of the shift and the needed spatial resolution with respect to the velocity field. When the size of the window increases, the noise is reduced as well as the number of independent measurements since each measurement is the average value on the whole window. The variation of surface state (due to vegetation growth, colluviums movement, anthropic modifications) is a factor that deeply influences the quality of the correlation. However, the correlation technique is less sensitive to surface changes than InSAR: on landslides, good correlations are reported using optical images acquired with a time frame of few years. Such a time interval is far too long for any accurate InSAR processing. Another problem occurs in the case of images acquired under different solar conditions. Some stable features will indeed present an apparent displacement in the correlation images because their shadow changed in size and direction [Berthier, 2005]. A good correlation is also difficult to obtain on forests because the signature of the different trees in the correlation window is redundant. The accuracy of this technique mainly depends on the quality of the projection of the two images in a common geometry, which implies a resampling of, at least, one image. The lower boundary for the displacement value is estimated at around 1/5 of the pixel size for satellite images and 2 or 3 pixels for aerial data (due to a stronger distortion of the optical images). The upper displacement value is not limited by the correlation technique but rather by the surface changes related to the displacement. Delacourt *et al.* [2004] have shown that displacements of up to 80 pixels can be measured.

Using this methodology, the projection of the local displacement vector in the focal plane of the sensor is measured. In the case of images acquired with vertical incidence angles (the most common case), the planimetric (horizontal) shift is measured. If the images are acquired with two similar but non-vertical incidence angles, the correlation is also sensitive to vertical displacements [Berthier *et al.*, 2006]. The vertical value of the displacement can be measured using two multi-temporal DEMs and the planimetric displacement components (fig. 4). The vertical displacement is equal to the difference between the elevation of a pixel on the oldest image and the elevation of the corresponding pixel on the youngest image, these elevations being measured on the corresponding DEM. In order to increase the precision of the measurement, the DEMs are adjusted by minimizing the vertical distance between the fixed areas. In that case, the precision of the vertical component depends on the relative precision of the DEMs, which is generally equal to the size of the pixel or better [Casson *et al.*, 2005].

A correlation of images acquired by different sensors can also be performed [Delacourt *et al.*, 2004]. Aerial images and high resolution Quickbird images of the “La Clapière” landslide have been successfully correlated despite their different geometry, in order to measure the velocity field of the landslide

The image correlation can also be applied to successive monoscopic images if they are acquired from the same position. The images must contain fixed points that can be used

as reference. The derived velocity field is not homogeneous in term of scale because the pixel sizes depend on their distance to the camera. The result of correlation therefore cannot be directly interpreted in term of velocity field.

DATASET, PLATFORMS AND SENSORS

Aerial images

The French territory is covered by aerial photographs since 1937 with a time span of about 5 years between two successive surveys, which are under the responsibility of IGN (the French National Geographic Institute). The photographs are taken using photogrammetric cameras on 24 cm by 24 cm negatives. The surface covered by a scene is about 5 by 5 km with an overlap of 60% on two adjacent scenes. The images can be scanned on a photogrammetric scanner, which limits the distortion to less than 1 per 10,000. The scan is generally performed at 1000 dots per inch (DPI) so that the resolution of the pixel is better than one meter. A DEM can be then built from two adjacent scenes using these digital scans, the internal parameters of the camera (focal length, position of fiducial marks, position of the camera principal point, distortion of the lenses) provided by IGN, and the absolute position of ground control points (GCP) measured in the field. Even for images characterized by poor radiometric dynamics, it is possible to build georeferenced DEMs at a resolution of one meter, and with a relative precision better than one meter [Casson *et al.*, 2003]. The corresponding orthorectified images are also built with a metric resolution and the 3D displacement field can thus be estimated with a metric precision in the worst cases. In the case of a 5 years time span, these images can successfully monitor landslides with a velocity of a half meter per year up to 16 meters per year, which corresponds to a displacement of 2.5 to 80 pixels.

In conclusion, the main advantages of the use of aerial images are the importance of the data archive (50 years of acquisition in France) and the resolution of the data that approaches 1 meter. The main disadvantage of this method is the poor temporal resolution in France. In order to improve this temporal resolution, dedicated mission can be planned, this solution being however expensive.

Optic satellites images

One way to overcome the limitations mentioned above is to use satellite images with a revisit period of 20 to 30 days. Until the beginning of the 21th century, the average spatial resolution of optical satellites (SPOT, LANDSAT) was decametric. Due to the small area extent of most of the Alpine landslides, those images were not suitable for landslide analysis. A new generation of high resolution satellites (Ikonos; QuickBird) provides high resolution (0.6 m to 1 m) data covering 10 km by 10 km areas. The SPOT5 satellite (launched on 4 May 2002) has a lower ground resolution (2.5 m) in Very High Resolution mode, but the wide footprint of 60 km by 60 km is useful for regional scale studies (fig. 5). Furthermore, precise orbital ephemeris and attitude descriptions are provided with the images. Without any GCP (Ground Control Points), an image is located on the ground with a precision of 30 m rms. Although Earth Observation satellites are sun synchronous, the change of

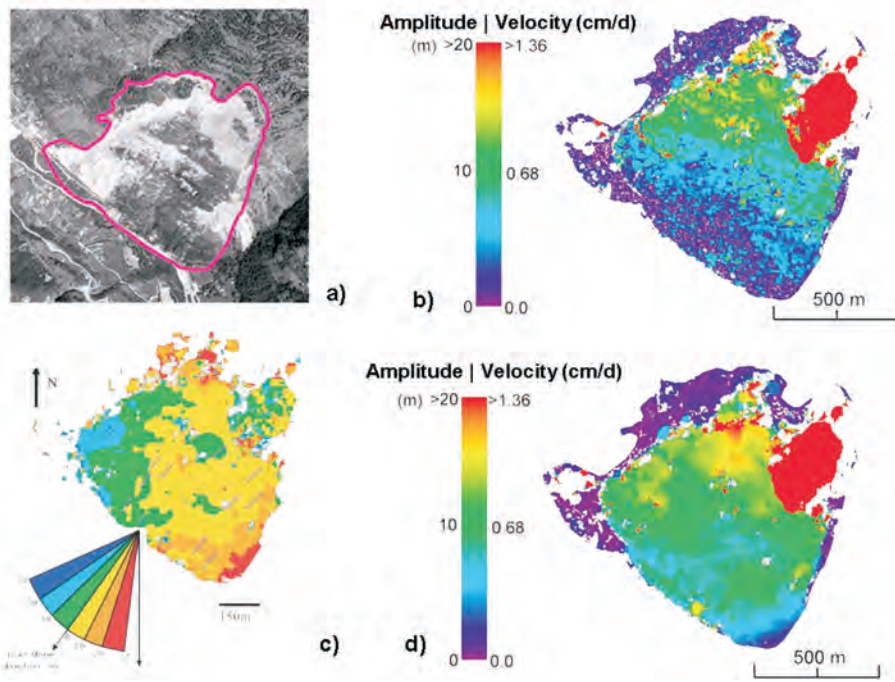


FIG. 4. – Displacement and velocity maps calculated using aerial image correlation (1995 – 1999) of “La Clapière” landslide. a) Aerial orthophotograph of the landslide. b) Horizontal velocity. c) Orientation displacement map in the horizontal plan. d) Vertical velocity map.

FIG. 4. – Cartes des déplacements et des vitesses de surface calculées par corrélation d’images aériennes (1995 – 1999) sur le glissement de terrain de “La Clapière”. a) Orthophotographie aérienne du glissement de terrain. b) Carte des vitesses horizontales. c) Carte de l’orientation du mouvement dans le plan horizontal. d) Carte des vitesses verticales.

Sun’s illumination between acquisitions can induce significant variation in the length and the direction of the shadows. In our example (fig. 5, first image taken on September, 19 2003, second image taken on August, 22 2004) the shadow of a 4 m high tree will lead to an apparent displacement of about 1.2 m (0.5 pixels) in the South-North direction, thus affecting the correlation in the line direction. The apparent displacement will even be stronger in the case of images acquired during different seasons.

Although the temporal resolution of satellite data is better than for aerial ones, the acquisition of images is fixed by orbital parameters. Moreover, for small and low velocity

landslides, metric spatial resolution and ~20 days temporal resolution is not always suitable. Additionally, the archive of high resolution satellites is very limited and cannot be used currently for general surveys at the scale of a massif, nor for a single landslide.

Remote-controlled platforms

Since the middle of the 90’s, the development of digital cameras equipped with sensors of more than 6M pixels and high quality lenses, has permitted the growth of new remote sensing technologies. Such cameras, which weight is less than 2 kg, can be installed onboard low-velocity drones or

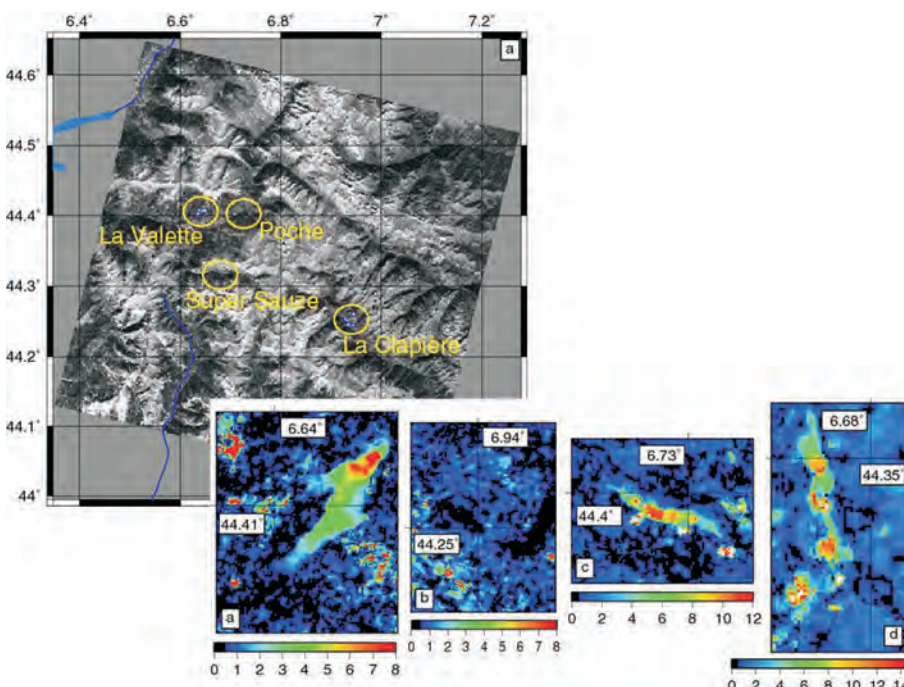


FIG. 5. – Horizontal displacement maps (m) over the French South Alps derived from the correlation of SPOT5 images (2003, 09/19 – 2004, 08/22). Three major landslides are clearly visible: a) “La Valette” mudslide, c) “Poche” mudslide and d) “Super Sauze” mudslide; b) “La Clapière” landslide is more difficult to discriminate.

FIG. 5. – Cartes des déplacements de surface (m) sur les Alpes françaises du Sud calculées à partir de la corrélation d’images SPOT5 (19/09/2003 – 22/08/2004). Trois glissements de terrain sont clairement visibles a) glissement-coulée de “La Valette”, c) glissement-coulée de “Poche” et d) glissement-coulée de “Super Sauze” ; b) glissement de terrain de “La Clapière”, plus difficilement détectable.

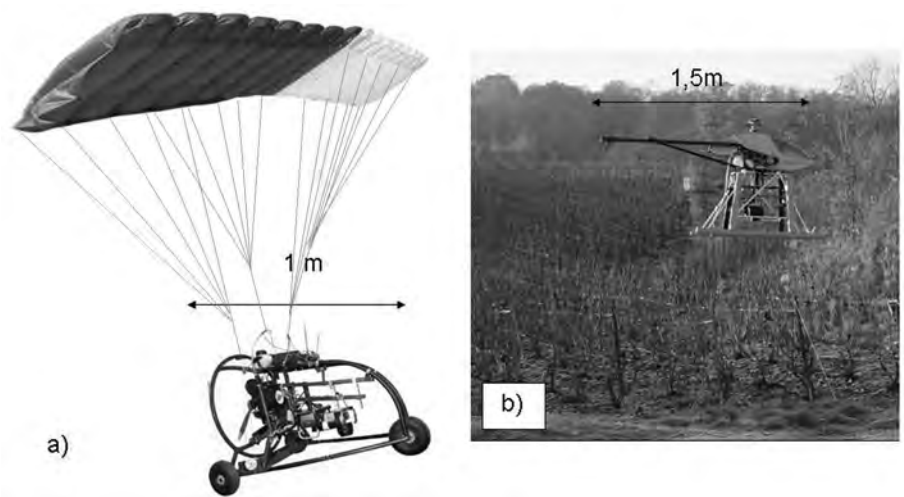


FIG. 6. – Remote-controlled platforms used. a) Drone.
b) Helicopter.
FIG. 6. – Plates-formes télécommandées utilisées.
a) Drone. b) Hélicoptère.

helicopters that are radio controlled from the ground (fig. 6) up to 2 km of distance from the operator. The drone is a two meters wingspan paramotor, which can fly at a low velocity (around 15 km.h^{-1}) and up to 600 m in altitude. This drone is very sensitive to atmospheric conditions and can fly only when the wind speed is below 20 km.h^{-1} . The helicopter is equipped with a 1.5 m diameter rotor and can fly up to 100 m with wind velocities up to 50 km.h^{-1} . The drone and the helicopter are equipped with a pendular mount on which the camera is fixed such that the line of sight of the camera is near the vertical. The drone and the helicopters are both equipped with GPS and video camera for good-quality positioning and navigation. The resolution of the images acquired in these conditions ranges 1 to 10 centimeters, and the surface covered by one image ranges 30 by 20 m to 400 by 250 m, depending on the flight altitude and on the quality of the camera optic. The quality of data indeed depends on the quality of the lenses, the velocity of the platform and the illumination conditions that controls the duration of the exposition. The images are generally acquired in sequences so that successive images are acquired with 70% of overlap. DEMs and orthophotographies can be constructed in a classical way using some GCP precisely positioned in an absolute reference frame. The factor limiting the precision of the DEM and the orthophotography is the positioning of the GCP, which have to be measured with a precision that is similar to the resolution of the image, in order to accurately estimate the position of cameras. Using differential GPS or tacheometric methods, it is possible to obtain a precision of 1 cm and 5 cm, respectively. As the imaged landslides have generally a surface larger than 300 by 200 m, it is necessary to mosaic some DEMs and orthophotographies to obtain a complete view of the landslides. The mosaicking procedure also induces errors, which are estimated at 2 to 5 pixels. Thus, the displacements measured by such a system have to be larger than 5 pixels to be outside the error bar, which correspond to absolute values of displacement of 5 to 50 cm. The main advantage of this system is that the data can be obtained with a frequency adapted to the landslide velocity and at a very high spatial resolution.

Fixed camera

The main problem of data sets acquired by flying platforms is that images cannot be obtained in exactly the same

geometry and that temporal resolution depends on flying conditions. The DEM construction requires that the position and the orientation of the cameras are computed from GCP. Digital cameras can be placed in front of landslides and programmed to take images with a constant time step. In that case, images are exactly in the same geometry and can be directly correlated. The precision of the correlation is controlled by a) the correlation algorithm, b) the movements of the camera due to thermal distortion, c) the change in the refraction indices of the atmosphere between the camera and the landslide and d) the change of sun illumination. The effect (a) is negligible as the correlation can be realized with a sub pixel accuracy. The second one (b) can be avoided if the camera is fixed on a rigid stand. Experiments show that (c) can produce apparent shift, up to 2 pixels, if the camera equipped with a 22 mm focal lens is placed at 1 km of the landslide. In order to minimize these artefacts, the images need to contain a stable area that will be used as a reference. As no displacement is expected within this area, the maximum displacement calculated using the correlation method will give an upper boundary for the error on the unstable domain. In order to reduce sun illumination effects, only the images obtained at the same time on two successive days are correlated with a preference for images acquired when the sun elevation is maximal. The correlation works also well on images acquired at the same solar time with one year interval.

Another problem comes from the size of the landslide compared to the image swath. Generally, only the lower part of the landslide can be imaged. There are also technical constraints inherent to these methods. Systems of image transmission need to be associated to the acquisition process in order to quickly process the data. Another problem is more conceptual: if no DEM is used, the resolution of the image depends on the distance between the landslide and the camera. Then, the displacement, which is evaluated in pixels by the correlation, cannot be translated in distance. This problem can be circumvented if a high spatial resolution DEM is available. This technique can be used to observe both very fast and very slow landslides, by adapting the time span between two acquisitions. Another strong constraint is the surface changes, which have to be low enough so that the correlation remains possible.

We have applied this method on the “La Clapière” landslide. A 6 million pixels numeric camera with a 22 mm focal length lens was emplaced at around 1 km of the landslide (fig. 7a). The images thus encompass the lower part of the structure and a stable area located in the northeast (fig. 7b). The acquisition was programmed every 30 minutes. On figure 7c we can see the displacements in lines between July, 22 2004 and September, 2 2005. As the camera is fixed in front of the landslide, the displacement mainly occurs in the image line direction. The eastern limit of the landslide is clearly visible and the estimation of the spatial variability of the motion can be achieved. In vegetated areas, the change of the surface state during the acquisition period masks the displacement component.

Terrestrial 3D laser scanner imaging

A 3D laser scanner is essentially a range finder that calculates the distance to an object point along a known trajectory in 3D space. It consists of an emitting diode that produces a laser source at a very specific frequency. Pulses are emitted at an extremely rapid rate while a rotating mirror in the head of the scanner reflects the light along different trajectories in a vertical plane. Simultaneously, the entire head of the scanner rotates in the horizontal plane thereby collecting data continuously [Riegl, 2004]. This system is combined with a calibrated and orientated high-resolution digital camera. The system used in this study is the RIEGL LMS-Z420i (laser scanner) and Nikon D100 (digital camera). This fully portable system provides both topography (laser) and photography (camera) with an accuracy better than 1 cm (+/- 20 part per million) and high spatial resolution (depending on the distance between the laser scanning and the target, in practice the maximal angular resolution is 0.004°). In order to cover a wide surface, different images have to be mosaicked. Depending on the backscattering conditions of the target, the maximum distance between the laser and landslide can reach 800 m. In wet conditions and on a landslide formed by black marls, this maximum distance is less than 400 m. This technique has been

successfully applied at the toe of the “La Clapière” landslide on a small 100 m by 100 m area. Three acquisitions have been performed in June 2003 (fig. 8a), October 2003 and October 2004 (fig. 8b). The changes in the vegetation affect the quality of data and prevent us to use the correlation technique on these photos. Nevertheless, due to the high sampling rate (one point each 25 cm² in average), 10% of the total points, free of vegetation, can be isolated to generate a DEM (fig. 9a). This DEM clearly exhibits various features that characterize landslides such as curved scarps. Eventually, multitemporal DEMs differences can be calculated (fig. 9b), revealing both depletion in the upper part of the area and accretion in the lower part.

CONCLUSION

Depending on the exposure conditions, the size and the velocity of landslides, as well as the goal of the study (operational or scientific purpose), one or a combination of several techniques and data (characterized by resolution, accuracy, covered surface, revisiting time) can be used [Array 1].

The aerial images obtained from the French IGN associated with image correlation are very useful for scientific studies of landslides that move at a rate of at least 25 cm/year. The archive of images encompasses 50 years with an average time span of 5 years between two acquisitions. The spatial resolution is equal or better than 1 m and the detection threshold is 2 or 3 pixels.

High resolution optical satellite images associated with image correlation techniques are useful for both scientific and hazard purposes. These images have a ground resolution around 1 m and the time span between 2 acquisitions is around 20 days, which can be reduced to 3 or 4 days in case of specific orbit cycles. Thus, these images are suitable for high velocity landslides (at least 1 m per day) if the time span is equal or less than 3 days. For medium velocity landslides (at least 2 or 3 meters per month) a time span of 20 days is required. They are suitable for low velocity landslides (2 or 3m per year) for a time span of one year. The

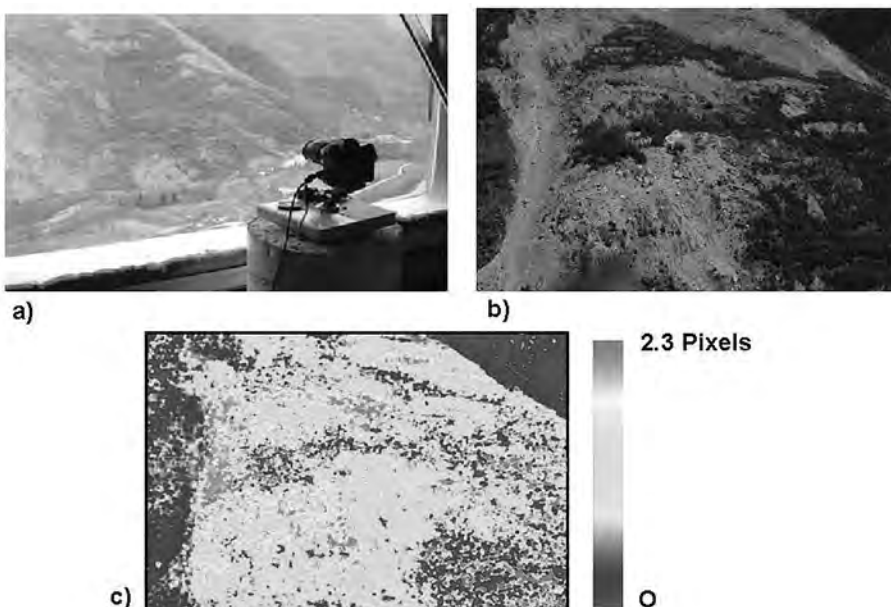


FIG. 7. – Displacement map of “La Clapière” landslide (in pixels) derived from fixed camera images. a) Fixed camera installed in front of the landslide. b) Photograph of 2005, 09/02. c) Total displacement in lines over the period 2004, 07/22 – 2005, 09/02.

FIG. 7. – Carte des déplacements de surface du glissement de terrain de “La Clapière” calculée par corrélation de photographies fixes. a) Appareil photographique et système d’acquisition. b) Photographie du 02/09/2005. c) Déplacement selon les lignes de l’image entre le 22/07/2004 et le 02/09/2005.

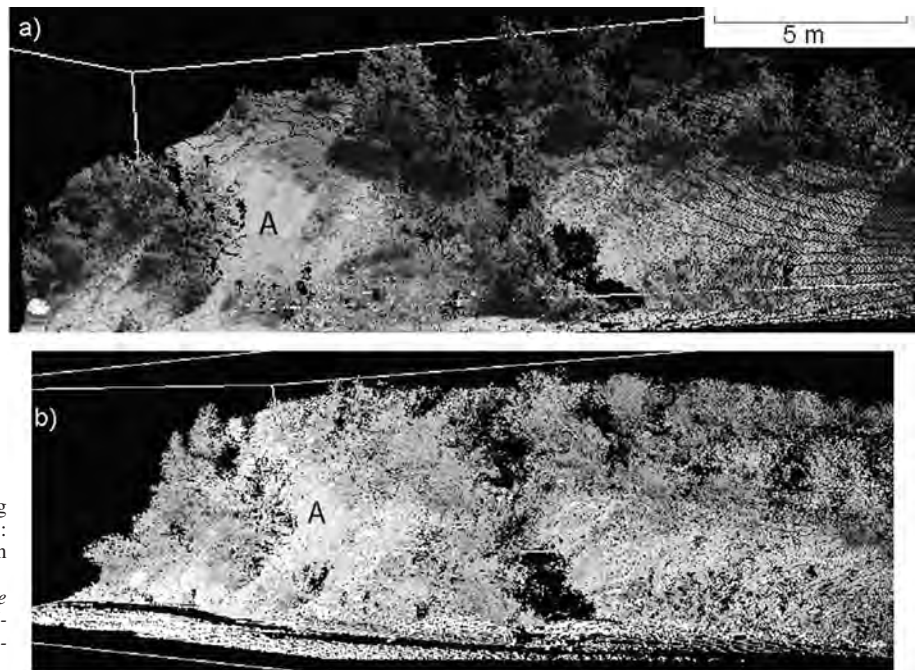


FIG. 8. – Terrestrial photogrammetric laser scanning images of the bottom of the “La Clapière” landslide: a) Image acquired in June 2003; b) image acquired in October 2004.

FIG. 8 – Images du pied du glissement de terrain de “La Clapière” acquises par laser photogrammétrique : a) image acquise en Juin 2003 ; b) image acquise en Octobre 2004.

archive of these images is however very limited (less than 6 years of record). High resolution images coming from different sensors can be combined.

Radar satellite data associated with interferometric techniques can be currently used only for scientific purpose. The archive is of 15 years for ERS-1 and ERS-2 satellites, 12 years for RADARSAT and 3 years for ENVISAT. However, images coming from different sensors cannot be combined (despite some difficulties for ERS and ENVISAT). The image resolution is about 20 m (3 m with the next generation of spaceborne sensors) in the most favourable case but

only part of mountainous regions can be analyzed. Displacements of the order of 1 to 4 cm can be detected along the line of sight of the satellite. Only moderate velocity landslides (1 to 4 cm per day) can be investigated using this method under the tree line when short time span data pairs are available. This is because the coherence between SAR images breaks down after a few days. The revisiting time spans of the presently available sensors (35 days for ERS-2 or ENVISAT) therefore constitute a limiting factor. In desert or unvegetated regions, very slow landslides (1cm per year) can be analyzed.

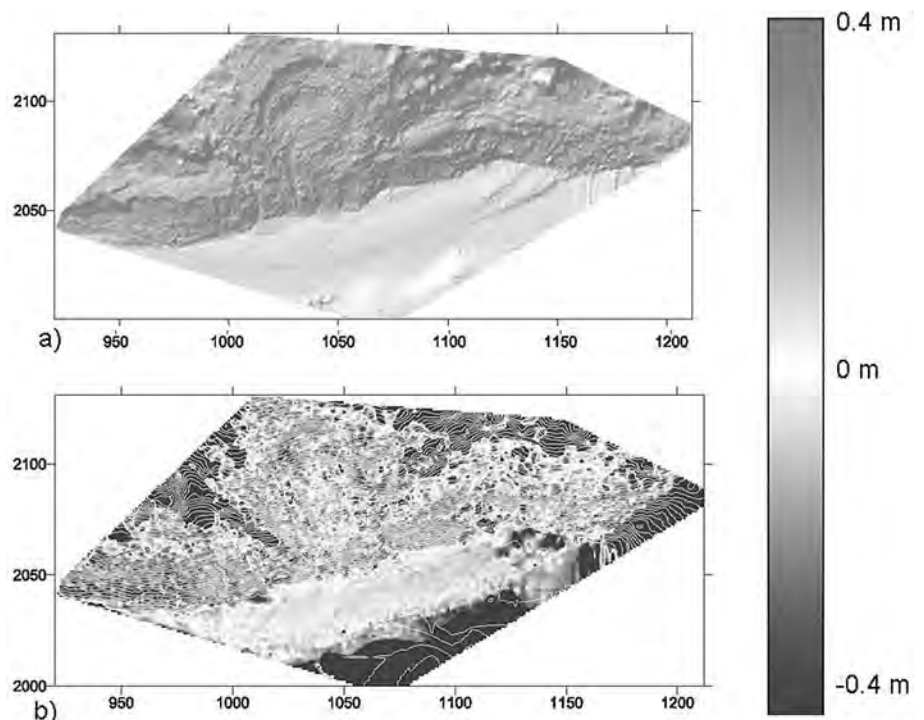


FIG. 9 – Information derived from terrestrial photogrammetric laser scanning at the toe of the “La Clapière” landslide. a) Digital Elevation Model (DEM). b) Differential DEM (September 2003 – October 2004).

FIG. 9. – Informations dérivées de levé laser photogrammétrique terrestre du pied du glissement de “La Clapière”. a) Modèle numérique de terrain (MNT). b) MNT différentiel (Juin 2003 – Octobre 2004).

Images acquired by unmanned platforms flying at low altitude can be used for both scientific and operational purposes. The archive of data depends only on the team in charge of a given landslide. Acquisition of data is sensitive to meteorological conditions. The reduced size of the surface that is covered by one image requires the use of image mosaics, which alters the accuracy of the positioning within large surfaces. So the detection threshold is high, about 5 pixels. However, every range of landslide velocities can be covered because of the very high resolution (1 to 10 cm) and the high adaptability of acquisition frequency.

Images acquired from fixed cameras can be used for both hazard and scientific purposes. The archive obviously depends on the considered landslide. The acquisitions cannot be treated in case of bad atmospheric or illumination conditions. The result of the correlation of these data is only qualitative if no DEM is available. Due to its high adaptability, each range of landslide velocities can be observed.

Terrestrial photogrammetric laser scan can be used for both scientific and hazard study on high slope landslides. The limited field of view makes the mosaicking of data necessary in order to cover a significant surface. Because of a very high spatial resolution, interpretation in term of global mass movement of the landslide is difficult. Thus, this technique needs further developments in terms of data processing.

Acknowledgements. – Support of this work was partially provided by the French National Institute of Universe (INSU) in the framework of the 'ACI – Prévention des Catastrophes Naturelles' Program (Project SAMOA). SAR Images were provided by the European Space Agency (ESA; CAT-1 1048). SPOT images were provided in the framework of the ISIS program of CNES. Radar interferometry analyses on "La Réunion Island" have been carried out with the support of the Research Direction of 'Bureau de Recherches Géologiques et Minières' (BRGM). Etienne Berthier thanks the European Union, which has supported part of this work through a Marie Curie Fellowship. Finally, the authors are grateful to two anonymous reviewers for their improvements of the manuscript.

References

- AMELUNG F., GALLOWAY D.L., BELL J.W., ZEBKER H. A. & LACCZNIAK R.J. (1999). – Sensing the ups and down of Las Vegas: InSAR reveals structural control of land subsidence and aquifer-systems deformation. – *Geology*, **27**, 483-486.
- ANGELI M.C., PASUTO A. & SILVANO S. (2000). – A critical review of landslide monitoring experiences. – *Eng. Geol.*, **55**, 133-147.
- ANTONELLO G., CASAGLI N., FARINA P., LEVA D., NICO G., SIEBER A.J. & TARCHI D. (2004). – Ground-based SAR interferometry for monitoring mass movements. – *Landslides*, **1**, 21-28.
- BARATOUX D., DELACOURT C. & ALLEMAND P. (2001). – High Resolution Digital Elevation Model derived from Viking images: New method and comparison with MOLA data. – *J. Geophys. Res.*, **106**, 32927-32942.
- BEAUDUCEL F., BRIOLE P. & FROGER J.L. (2000). – Volcano wide fringes in ERS SAR interferograms of Etna: Deformation or tropospheric effect? – *J. Geophys. Res.*, **105**, 16391-16402.
- BERTHIER E. (2005) – Dynamique et bilan de masse des glaciers de montagne (Alpes, Islande, Himalaya). Contribution de l'imagerie satellitaire. – PhD Thesis, Univ. Paul Sabatier., 250 p.
- BERTHIER E., BJÖRNSSON H., PÁLSSON F., FEIGL K. L., LLUBES M. & RÉMY F. (2006). – The level of the Grimsvötn subglacial lake, Vatnajökull, Iceland, monitored with SPOT5 images. – *Earth Planet. Sci. Lett.*, **243**, 293-302.
- BERTHIER E., VADON H., BARATOUX D., ARNAUD Y., VINCENT C., FEIGL K.L., RÉMY F. & LEGRÉSY B. (2005). – Mountain glaciers surface motion derived from satellite optical imagery. – *Remote Sens. Environ.*, **95**, 14-28.
- CARNEC C., MASSONNET D. & KING C. (1996). – Two examples of the use of SAR interferometry on displacement fields of small spatial extent. – *Geophys. Res. Lett.*, **23**, 3579-3582.
- CASSON B., BARATOUX D., DELACOURT C. & ALLEMAND P. (2003). – "La Clapière" landslide motion observed from aerial differential high resolution DEM. – *Eng. Geol.*, **68**, 123-139.
- CASSON B., DELACOURT C. & ALLEMAND P. (2005). – Contribution of multi-temporal remote sensing images to characterize landslide slip surface – Application to the "La Clapière" landslide (France). – *Nat. Haz. Earth Sys. Sc.*, **5**, 425-437.
- COLESANTI C., LE MOUËLIC S., BENNANI M., RAUCOULES D., CARNEC C. & FERRETTI A. (2003a). – Detection of mining related ground instabilities using the permanent scatterers technique – A case study in the East of France. – *Intern. J. Remote Sens.*, **1**, 201-207.
- COLESANTI C., FERRETTI A., NOVALI C., PRATI C. & ROCCA F. (2003b). – SAR monitoring of progressive and seasonal ground deformation using the Permanent Scatterers Technique. – *IEEE Trans. Geosci. Remote Sens.*, **41**, 1685-1701
- COLESANTI C., FERRETTI C., PRATI C. & ROCCA F. (2003c). – Monitoring landslide and tectonics motions with the permanent scatterers technique. – *Eng. Geol.*, **68**, 3-14.
- DELACOURT C., BRIOLE P. & ACHACHE J. (1998). – Tropospheric corrections of SAR interferograms with strong topography. Application to Etna. – *Geophys. Res. Lett.*, **25**, 2849-2852.
- DELACOURT C., ALLEMAND P., SQUARZONI C., PICARD F., RAUCOULES D. & CARNEC C. (2003). – Potential and limitation of ERS-Differential SAR Interferometry for landslide studies in the French Alps and Pyrenees. – *Proc. Fringe 2003*, Frascati, Italy, ESA-ESRIN. Available at: <http://earth.esa.int/fringe03/proceedings/>
- DELACOURT C., ALLEMAND P., CASSON B. & VADON H. (2004). – Velocity field of the "La Clapière" landslide measured by the correlation of aerial and QuickBird satellite images. – *Geophys. Res. Lett.*, **31**, L15619, 10.1029/2004GL020193.
- FERRETTI A., PERISSIN D., PRATI C. & ROCCA F. (2004). – ERS-ENVISAT permanent scatterers. – *Proc. IGARSS 2004*, Anchorage, Canada, Vol. 2, 985-988.
- FERRETTI A., PRATI C. & ROCCA F. (2001). – Permanent scatterers in SAR Interferometry. – *IEEE Trans. Geoscience Remote Sens.*, **39**, 8-20.
- FIALKO Y., SANDWELL D., SIMONS M. & ROSEN P. (2005). – Three-dimensional deformation caused by the Bam, Iran, earthquake and the origin of shallow slip deficit. – *Nature*, **435**, 295-299.
- FOLLACCI J.-P., GUARDIA P. & IVALDI J.-P. (1988). – Geodynamic framework of "La Clapière" landslide (Maritime Alps, France). – *Proc. 5th International Symposium on Landslides*, Lausanne, Suisse, Vol. 2, 1323-1327.
- FRUNEAU B., ACHACHE J. & DELACOURT C., (1996). – Observation and modelling of the Saint-Étienne-de-Tinée landslide using SAR interferometry. – *Tectonophysics*, **265**, 181-190.
- GILI J.A., COROMINAS J. & RIUS J. (2000). – Using global positioning system techniques in landslide monitoring. – *Eng. Geol.*, **55**, 167-192.
- GOLDSTEIN R. M., ENGLEHARDT H., KAMB B. & FROLICH R.M. (1993). – Satellite radar interferometry for monitoring ice sheet motion: Application to an Antarctic Ice Stream. – *Science*, **262**, 525-530.
- HILLEY G.E., BÜRGMANN R., FERRETTI A., NOVALI F. & ROCCA F. (2004). – Dynamics of slow-moving landslides from permanent scatterers analysis. – *Science*, **304**, 1952-1955.

- JACKSON M.E., BODIN P.W., SAVAGE W.Z. & NEL E.M. (1996). – Measurement of local velocities on the Slumgullion landslide using the global positioning system. *In*: D.J. VARNES, W.Z. SAVOGE, Eds, the Slumgullion earthflow: a large scale natural laboratory. – *U.S. Geol. Surv. Bull.*, **2130**, 93-95.
- KÄAB A. (2002). – Monitoring high-mountain terrain deformation from repeated air- and spaceborne optical data: examples using digital aerial imagery and ASTER data. – *ISPRS J. Photogramm. Remote Sens.*, **57**, 39-52.
- KÄAB A., HUGGEL C., FISCHER L., GUE, S., PAUL F., ROER I. & SALZMANN N. (2005). – Remote sensing of glacier- and permafrost-related hazards in high mountains: An overview. – *Nat. Haz. Earth Sys. Sc.*, **5**, 527-554.
- KIMURA H & YAMAGUCHI Y. (2000). – Detection of landslide areas using satellite radar interferometry. – *Photogram. Eng. Remote Sens.*, **66**, 337-344.
- MALET J.-P., MAQUAIRE O. & CALAIS E. (2002). – The use of global positioning system techniques for the continuous monitoring of landslides. – *Geomorphology*, **43**, 33-54.
- MASSONNET D., ROSSI M., CARMONA C., ADRAGNA F., PELTZER G., FEIGL K. & RABAUTE T. (1993). – The displacement field of the Landers earthquake mapped by radar interferometry. – *Nature*, **364**, 138-142.
- MASSONNET D., BRIOLE P. & ARNAUD A. (1995). – Deflation of Mount Etna monitored by spaceborn radar interferometry. – *Nature*, **375**, 567-570.
- MASSONNET D. & FEIGL K. (1998). – Radar interferometry and its applications to changes in the earth's surface. – *Rev. Geophys.*, **36**, 441-500.
- NAGLER T., MAYER C. & ROTT H. (2002). – Feasibility of DInSAR for mapping complex motion fields of Alpine ice and rock glaciers. – *Proc. 3rd International Symposium on Retrieval of Bio- and Geophysical Parameters from SAR Data for Land Applications*, Sheffield, UK, ESA SP-475, 377-382.
- RAUCOULES D., CRUCHET M., DELACOURT C., CARNEC C., FEURER D. & LE MOUELIC S. (2006). – Characterization of landslides in La Réunion Island with JERS and Radarsat radar interferometry. – *Eng. Geol.* (in press).
- REMI D. (2005). – Analyse et inversion de séries interférométriques et microgravimétriques temporelles sur les volcans actifs: apport à la quantification d'effets de sites et à la compréhension de la dynamique volcanique. – PhD Thesis, Institut de Physique du Globe de Paris, 250 p.
- RIEGL Cie. (2004). – Laser measurement systems GmbH – Technical data at www.riegl.com
- ROTT H., SCHEUCHL B., SIEGEL A. & GRASEMANN B. (1999). – Monitoring very slow slope motion by means of SAR interferometry: A case study from a mass waste above a reservoir in the Ötztal Alps, Austria. – *Geophys. Res. Lett.*, **26**, 1629-1632.
- SCAMBOS T.A., DUTKIEWICZ M.J., WILSON J.C. & BINDSCHADLER R.A. (1992). – Application of image cross-correlation to the measurement of glacier velocity using satellite image data. – *Remote Sens. Environ.*, **42**, 177-186.
- SCHREIER G. (1993). – SAR Geocoding: Data and systems. – Wichmann Ed., Karlsruhe, 435 p.
- SQUARZONI C., DELACOURT C. & ALLEMAND P. (2003). – Nine years of spatial and temporal evolution of the La Valette landslide observed by SAR interferometry. – *Eng. Geol.*, **68**, 53-66.
- STROZZI T., WEGMULLER U., WERNER C., WIESSMANN A. & SPRECKELS V. (2003). – JERS SAR interferometry for land subsidence monitoring. – *IEEE Trans. Geoscience & Remote Sens.*, **7**, 1702-1707.
- STROZZI T., KÄAB A. & FRAUENFELDER R. (2004). – Detecting and quantifying mountain permafrost creep from in situ inventory, space-borne radar interferometry and airborne digital photogrammetry. – *Int. J. Remote Sens.*, **25**, 2919-2931.
- STROZZI T., FARINA P., CORSINI A., AMBROSI C., THÜRING M., ZILGER J., WIESSMANN A., WEGMÜLLER U. & WERNER C. (2005). – Survey and monitoring of landslide displacements by means of L-band satellite SAR interferometry. – *Landslides*, **2**, 193-201.
- TARAYRE H. & MASSONNET D. (1996). – Atmospheric propagation heterogeneities revealed by ERS-1 interferometry. – *Geophys. Res. Lett.*, **23**, 989-992.
- VADON H. & MASSONNET P. (2000). – Earthquake displacement fields mapped by very precise correlation. Complementarity with radar interferometry. – *Proc. IGARSS 2000*, New-York, USA, Vol. 6, 2700-2702.
- VAN PUYMBROECK N., MICHEL R., BINET R., AVOUAC J.-P. & TABOURY J. (2000). – Measuring earthquakes from optical satellite images. – *Applied Optics*, **39**, 3486-3494.
- ZEBKER H.A. & GOLDSTEIN R.M. (1985). – Topographic mapping from interferometric synthetic aperture radar observations. – *Proc. IGARSS 1985*, Amherst, USA, Vol. 1, 113-117.
- ZEBKER H.A. & VILLASENOR J. (1992). – Decorrelation in interferometric radar echoes. – *IEEE Trans. Geoscience & Remote Sens.*, **30**, 950-959.
- ZEBKER H. A., ROSEN P., GOLDSTEIN R.M., GABRIEL A. & WERNER C.L. (1994). – On the derivation of coseismic fields using differential radar interferometry: The Landers earthquake. – *J. Geophys. Res.*, **99**, 19617-19634.
- ZINK M. (2003). – The TerraSAR-L interferometric mission objectives. – *Proc. Fringe 2003*, Frascati, Italy, ESA-ESRIN. Available at: <http://earth.esa.int/fringe03/proceedings/>